CFD, System-Based, and EFD Preliminary Investigation of ONR Tumblehome Instability and Capsize with Evaluation of the Mathematical Model

Hamid Sadat-Hosseni[1], Motoki Araki[2], Naoya Umeda[2], Masaaki Sano[3], Dong Jin Yeo[4], Yasuyuki Toda[2], Pablo M. Carrica[1], Frederick Stern[1]

[1]*IIHR - Hydroscience & Engineering, The University of Iowa,USA*
[2]*Department of Naval Architecture and Ocean Engineering, Osaka University, Japan*
[3]*Department of Transportation and Environmental System, Graduate School of Engineering, Hiroshima University, Japan*
[4]*Maritime & Ocean Engineering Research Institute (MOERI), South Korea*

ABSTRACT

CFD and 4DOF system-based are performed for free-running ONR Tumblehome for turning circle and zigzag maneuvering in calm water and waves. The preliminary results are validated against experiments executed in IIHR wave basin and investigated with consideration to the mathematical model of ship motions. The maneuvering coefficients are predicted by sign constrained least square method using CFD outputs to evaluate the mathematical model in component level and in overall. The CFD and system-based time histories show fairly good agreement with experiment. The estimated maneuvering coefficients from the sign constrained least square method show some discrepancy from experimental data. In future, the CFD model will be improved adding all appendages and possibly the discretized propellers. The system-based also will be improved for wave forces. In addition, other types of calm water maneuvering such as random/sinusoidal rudder deflection tests which might help avoiding simultaneous drift problem should be used for system identification. Moreover, better system identification techniques such as extended Kalman filtering will be taken into account to accurately estimate the maneuvering coefficients from CFD outputs in calm water and then from more complicated cases such as broaching in waves.. For EFD, the release system and local flow measurement system will be installed to improve the tests. Also, the stability of the tracking system will be investigated and enhanced.

KEYWORDS

CFD; EFD; System-Based; Turning Circle Test; Zigzag Test; System Identification; Constrained Least Square Method.

INTRODUCTION

Nowadays there are two major simulation methods for prediction of ship instability and capsize: system-based (SB) and computational fluid dynamics (CFD). Despite the progress achieved in SB, the mathematical model needs to be improved. Yasukawa (2006b) designed 6DOF system-based maneuvering model for general wave conditions to predict turning and zigzag in waves. The simulations showed only qualitative agreements with EFD and had some difficulties for quantitative prediction in wave conditions. Umeda et al. (2008) developed 4DOF system-based broaching model for following waves with low encounter frequency to predict the instability map for ONR Tumblehome for varying heading and speed. The model showed qualitative agreement but the predicted roll exceeds 90° for Fr>0.3 while EFD maximum roll angle is 71°. On the contrary, CFD showed ability to predict quantitatively ship instability and capsize in waves such as parametric roll and broaching

(Sadat-Hosseni et al., 2010, 2011). Since both state variables and forces/moments are predicted, the validated CFD predictions provided an opportunity to study the mathematical model in system-based simulations. For parametric roll the mathematical model was derived and investigated in overall and in component level. However, the derived mathematical model for broaching could not be investigated due to extreme complexity of the problem.

The object of this paper is to study the mathematical model first for less complicated cases such as turning circle and zigzag in calm water and waves and then for more complicated cases such as broaching. The preliminary CFD outputs i.e. state variables and forces/moments are used to investigate the mathematical model and to evaluate the maneuvering coefficients using system identification technique (Abkowitz, 1980), in which the maneuvering coefficients are predicted by using the state variables from EFD or CFD free-running trials. The sign constrained least square method is used to fit the predicted forces/moments to the mathematical model.

EFD METHOD

The construction of the new IIHR wave basin (Fig. 1) for ship hydrodynamics was completed in August 2010. Preliminary and wave-maker calibration tests were completed through early spring 2011 and the present experiments initiated soon thereafter. The wave basin is 40×20 square meter with 3-meters water depth and designed to test captive or radio-controlled model scale ships, under a variety of wave conditions, created by the basin's six plunger-type wave makers. All of EFD data was acquired in this new facility. The 1/49 scaled model of ONR tumblehome (Table 1) appended with skeg and bilge keels was used. The model also had rudders, shafts and propellers with propeller shaft brackets.

Roll, pitch and yaw angles were measured by FOG gyro. The accuracy of roll and pitch angles was $\pm$0.5 deg, while that for yaw angle was $\pm$1.0 deg without considering the error due to so called drift. The amount of drift of yaw angle can be kept $\pm$1.0 deg/5min on the average if the accumulative amount of drift is reset at regular time interval, i.e., about 10 minutes.

The number of propeller revolutions (rpm) was counted by a photo micro sensor and the rudder angle was estimated from the number of pulse signals transmitted to the rudder-driving stepping motor. Every data of the free-running system was recorded with a frequency of by 20 Hz. Meanwhile, the plane trajectory of model ship was recorded with a frequency of 10 Hz by the tracking system. A sub-carriage hanging by the overhead main carriage tracks the radio-controlled ship using the two-camera vision. The tracking cameras catch two LED lights placed on the deck of model ship. The mid-point of two LEDs corresponds to the longitudinal center of gravity (LCG) of the model ship, but 0.191 m higher than the vertical CG point due to space restriction. Model ship's horizontal positions can be indirectly estimated by monitoring the rotational speed of each direction-motor. The maximum tracking speeds in the longitudinal (x) and transverse (y) directions are 2.5 m/s, while for the rotational speed it is 60 deg/s. The accuracies are better than $\pm$0.1 m for x and y and $\pm$8 deg for rotation. Although the free-running and tracking systems are fully independent, all data can be synchronized receiving the start-signal of radio control simultaneously. In terms of wave measurement, one capacitance type wave probe was set close at the wave makers and waves were measured with a frequency of 100 Hz. The data was used for estimating the wave phase at the LCG position of model ship just when the ship started maneuvering.

The experimental procedure was as follows. The model was held parallel to carriage rail. When propellers of the model started to rotate, model was pushed by hand to assist the initial acceleration. It was required because the size of the wave basin is not long enough to get desired speed before maneuvering command starts. But there still were difficulties in getting the target initial speed, so each test was repeated several times. A launching system will be available soon and, make it possible to get the target initial speed more effectively. After launching, the ship advanced straight without any rudder deflection for a specified period and started maneuvering after pre-set time. Propeller rpm was kept constant while running. About one and half turnings were recorded in turning test. As for zigzag test, when

the ship approached to the wave makers, operator stopped the test. With the available running distance 2nd overshoot angles could be measured for each test. Regarding tests in waves, we tried to launch the ship after the wave train propagated over the half of wave basin.

a)

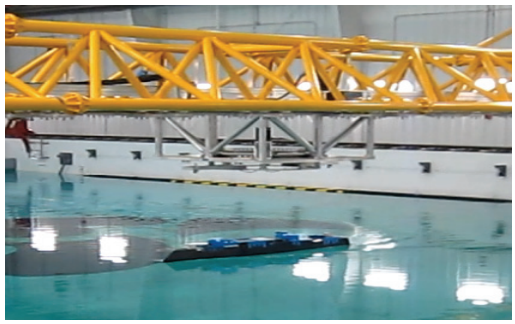

b)

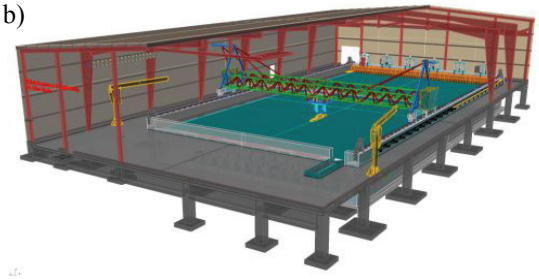

Fig.1 EFD setup; a: Installation of the model, carriage and sub-carriage, b: Drawing of IIHR wave basin

SYSTEM-BASED METHOD

The 4-DoF system-based broaching model developed by Umeda et al. (2000) is used for system-based simulations. Horizontal body axes are used for coordinate system. Also, Fujii's rudder model (1961), shown in equations (1)-(3), is used to implement rudder forces/moments.

$$F_N = \frac{1}{2}\rho A_R U_R^2 f_\alpha \cdot \sin\alpha_R \tag{1}$$

$$f_\alpha = \frac{6.13\Lambda_R}{\Lambda_R + 2.25} \tag{2}$$

$$\alpha_R = \delta - \gamma_R\left(\frac{U}{u_R}\right)(\beta - l_R' r') \tag{3}$$

Two types of 4-DoF system-based models are presented herein. One is a linear coupled surge-sway-roll-yaw mathematical model (SB-L) and the other one is a nonlinear coupled surge-sway-roll-yaw mathematical model (SB-NL), as shown in Eqs. (4)–(7) and Eqs. (8)–(11), respectively.

Table 1 Principal particulars of the ONR tumblehome vessel

Parameter	Model scale
Length: L	3.147 m
Breadth: B	0.384 m
Depth: D	0.266 m
Draft: d	0.112 m
Displacement: W	72.6 kg
Metacentric height: GM	0.0422 m
Natural roll period: T_ϕ	1.665 s
Rudder area: A_R	0.012 m^2 × 2
Block coefficient: C_b	0.535
Radius of gyration in pitch: κ_{yy}	0.246 × L
Maximum rudder angle: δ_{max}	± 35°

In both models, resistance and propeller thrust are estimated from a captive model experiment and a propeller open water test in calm water as described in Umeda et al (2008). Roll restoring moment, *mgGZ*, is estimated from hydrostatic calculation in calm water. Maneuvering coefficients and heel-induced hydrodynamic derivatives are estimated from calm water captive model experiments (Hashimoto et al., 2008). Roll damping is estimated from roll decay model tests (Umeda et al. 2008). Rudder forces include the effect of wave particle velocity. For ONR tumblehome vessel, flow-straightening effect coefficients γ_R, shown in Eq. (3), is adjusted to 0.60 as the rudders are situated far from the hull compared to other conventional ships. Thus the flow-straightening effect caused by body hull would be smaller i.e. the effect of sway and yaw on the rudders would be larger. The Froude-Krylov forces are calculated by integrating the water pressure around the submerged hull surface. A slender ship theory for zero encounter frequency is used for diffraction forces in sway, roll and yaw. Note that this model is designed for low encounter frequency conditions such as following and quartering waves and is not accurate for head waves. This is because our ultimate goal is to predict instability in following

and quartering waves, which are relevant to safety of the subject ship.

$$(m+m_x)\dot{u} = T(u;n) - R(u) + X_R(\delta,\xi_G/\lambda,\psi,u,v,r) + X_w(\xi_G/\lambda,\psi) \quad (4)$$

$$(m+m_y)\dot{v} + (m+m_x)ur = Y_v(u)v + Y_r(u)r + Y_\phi(u)\phi + Y_R(\delta,\xi_G/\lambda,\phi,\psi,u,v,r) + Y_w(\xi_G/\lambda,\psi,u) \quad (5)$$

$$(I_{xx}+J_{xx})\dot{p} = m_x z_H ur + K_v(u)v + K_r(u)r + K_p(u)p + K_\phi(u)\phi - mgGZ(\phi) + K_R(\delta,\xi_G/\lambda,\psi,u,v,r) + K_w(\xi_G/\lambda,\psi,u) \quad (6)$$

$$(I_{zz}+J_{zz})\dot{r} = N_v(u)v + N_r(u)r + N_\phi(u)\phi + N_R(\delta,\xi_G/\lambda,\phi,\psi,u,v,r) + N_w(\xi_G/\lambda,\psi,u) \quad (7)$$

$$(m+m_x)\dot{u} = T(u;n) - R(u) + X_R(\delta,\xi_G/\lambda,\psi,u,v,r) + X_w(\xi_G/\lambda,\chi) + X_{vr}(u)vr + X_{rr}(u)r^2 + X_{vv}(u)v^2 \quad (8)$$

$$(m+m_y)\dot{v} + (m+m_x)ur = Y_v(u)v + Y_r(u)r + Y_\phi(u)\phi + Y_R(\delta,\xi_G/\lambda,\phi,\psi,u,v,r) + Y_w(\xi_G/\lambda,\psi,u) + Y_{vvv}(u)v^3 + Y_{vvr}(u)v^2r + Y_{vrr}(u)r^2v + Y_{rrr}(u)r^3 \quad (9)$$

$$(I_{xx}+J_{xx})\dot{p} = m_x z_H ur + K_v(u)v + K_r(u)r + K_p(u)p + K_\phi(u)\phi - mgGZ(\phi) + K_R(\delta,\xi_G/\lambda,\psi,u,v,r) + K_w(\xi_G/\lambda,\psi,u) + K_{vvv}(u)v^3 + K_{vvr}(u)v^2r + K_{vrr}(u)r^2v + K_{rrr}(u)r^3 \quad (10)$$

$$(I_{zz}+J_{zz})\dot{r} = N_v(u)v + N_r(u)r + N_\phi(u)\phi + N_R(\delta,\xi_G/\lambda,\phi,\psi,u,v,r) + N_w(\xi_G/\lambda,\psi,u) + N_{vvv}(u)v^3 + N_{vvr}(u)v^2r + N_{vrr}(u)r^2v + N_{rrr}(u)r^3 \quad (11)$$

CFD METHOD

CFDShip-Iowa v4 (Carrica et al., 2010) is used for the CFD computations, which is an overset, block structured CFD solver designed for ship applications using either absolute or relative inertial non-orthogonal curvilinear coordinate system for arbitrary moving but non-deforming control volumes. Turbulence models include blended k-ε/k-ω based isotropic and anisotropic RANS, and DES approaches with near-wall or wall functions. A single-phase level set method is used for free-surface capturing. Captive, semi-captive, and full 6DOF capabilities for multi-objects with parent/child hierarchy are available. Numerical methods include advanced iterative solvers, higher order finite differences with conservative formulation, PISO or projection methods for pressure-velocity coupling, and parallelization with MPI-based domain decomposition. Dynamic overset grids use SUGGAR to compute the domain connectivity. The free-running model is appended with skeg and bilge keels and twin rudders mimicking the EFD conditions but not appended with propeller shaft brackets, propeller shafts and actual propellers. The propellers are modelled as a body force applied at a disk volume. This body force uses radial distribution. The rudders are modelled as a child object to the ship, and the deflection is controlled through a controller similar to EFD. Maximum rudder deflection and deflection rate are also specified as in EFD.

RESULTS

Speed Test

In the CFD, the open water curves are input for body force propeller model as a second order polynomial fit of the experimental $K_T(J)$ and $K_Q(J)$ curves, with the advance coefficient computed using the ship speed, thus neglecting the wake effects. Then the required propeller RPS at each Froude number is predicted with a 2DOF sinkage and trim simulation in calm water with a speed controller set at the desired Froude number. The resulting RPS is later prescribed in free model simulations in waves. It must be stressed that this propeller model is the simplest that can be applied and has some significant limitations. The most important is that the thrust and torque do not depend on the local flow field near the propellers, but on the average velocity of the ship. In addition, the body force is axisymmetric and side forces are neglected. Serious restrictions on the ability of the propeller model to handle strongly unsteady flows can also be expected. In SB models, RPS is predicted from open water curves similar to CFD. Also, the wake effect and side forces are neglected in SB model. Fig. 2 shows the results of EFD, CFD and SB speed test. The CFD and SB RPM are less than 1% different at Fr = 0.10 and 0.20 but the error between CFD and EFD is 9% at Fr = 0.10 and Fr = 0.20. This discrepancy is likely due to the non-interactive nature of the propeller model that neglects the boundary layer and thus results in higher advance velocities and higher rotational speeds to achieve the same thrust. Also the omitted appendages in CFD model might produce part of this error.

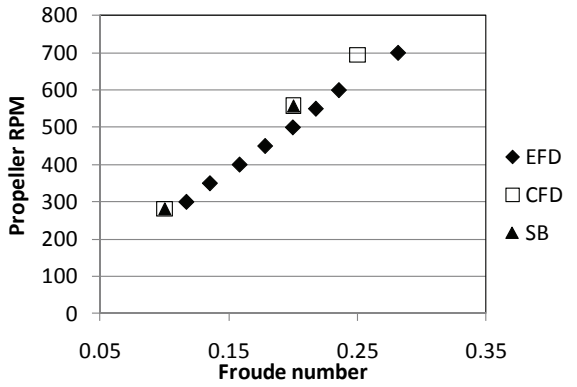

Fig.2 EFD, CFD and SB comparison of propeller RPM in speed test

Zigzag and Turning Circle

The EFD, CFD and SB cases for maneuvering in calm water and waves are listed in Table 2. The results for turning circle in calm water are shown in Fig.3a-d. The turning diameters and the comparison errors are listed in Table 3. The SB-NL trajectories show good agreement with experiment while SB-L under predicts the turning diameter as the nonlinearity is not considered. CFD also shows smaller turning diameter and the comparison error with EFD is in the range of 7-22%. In fact, the CFD turning rate is larger than that in EFD which is probably due to not including the shaft brackets in the CFD model and the grid quality. Other computations (Carrica et al., 2011) performed for DTMB-5415 at Fr=0.25-0.41 show that the errors between CFD and experiments are within 10% accuracy. The simulations were performed using the same body force propeller model for the ship model appended with bilge keels, roll stabilizer fines, twin rudders, and shafts and shaft brackets. Therefore there is a chance to reduce the discrepancy for current simulations by adding all appendages. The time series of the turning circle test in calm water with nominal Fr = 0.20 and δ = 35 deg are shown in Fig.4. CFD and SB-NL predict the speed drop due to large rudder deflection as shown in Fig. 4a. However, both over predict slightly the steady state ship speed which is probably due to the body force propeller model. Figures 4b and 4c show the sway and yaw rate histories predicted by CFD and SBs. The rate of increase of the sway and yaw rate at the beginning of the turn maneuver are closely matched by CFD and SBs but not for the time when EFD reaches to a steady value. The SB-L over predicts the steady value indicating that the nonlinear maneuvering coefficients in SB-NL like Y_{vvv} , N_{rrr}, shown in Eq. (9) and (11), are necessary for the large maneuvers such as turning circle tests. CFD also over predicts the sway and yaw rate as the counteracting yaw moment induced by shaft brackets are not included.

Figure 4d depicts roll angle time histories. CFD and SB-L over predict the steady roll angle as both under predict the turning diameter. Note that the roll angle is dominated by centripetal acceleration, proportional to the square of the velocity and inversely proportional to the radius. Overall SB-NL shows the best and SB-L shows the worst agreement with EFD. The CFD results possibly will be improved by adding all appendages and using finer grid. Figures 5a-d show the trajectories of zigzag tests in calm water. Note that the EFD trajectories have some errors because of the drift-effect of FOG gyro and possibly the misalignment of initial heading direction at launching. The results indicate that both SB-NL and SB-L predict similar trajectory. However, the CFD model overshoots more than the experiment due to less yaw damping.

Figure 6 shows the time series of the 20/20 zigzag test in calm water with nominal Fr = 0.20. The results show that the CFD tends to under predict the roll and yaw damping resulting in overshooting heading and over predicting roll angle. The damping under prediction might be due to not including shaft brackets and/or in part be due to the simplistic propeller model that neglects side forces and moments that tend to damp roll and other motions. The SB-NL shows very good agreement with EFD but overestimates the roll angle. This could be due to the fact that the SB-NL model does not include the term related to sway acceleration in the roll equation and sway accelerations are not so small for cases with large rudder deflection. SB-L overestimates all state variables indicating that SB model needs nonlinear terms for such large maneuvers.

The ship maneuverability can be defined by steering quality indices K and T estimated from zigzag test (Nomoto et al., 1956). Figure 7 shows K and T estimated from 20/20 zigzag test with

nominal Fr = 0.20. CFD and SB-L show larger rotational index K i.e. the rudder turning moment is over predicted and/or yaw damping is underestimated causing the smaller turning diameters during turning circle tests. For index T, CFD shows large discrepancy with EFD and other models i.e. yaw damping is significantly under predicted.

Figure 8 shows the turning circle and zigzag tests trajectories in waves. In Fig.8a, EFD shows the turning circle shifted to negative x direction compared to calm water cases because of the wave drift forces. However both SB-NL and SB-L trajectories do not show any shift as SB models do not include any of the wave drift force terms. This shifting could be reproduced by adding wave drifting terms in SB models. The initial surge velocity for CFD is zero and not the same as EFD such that the wave drift effect cannot be confirmed from the first turning circle and CFD simulation should have been continued for one more turning circle to reach conclusions. The turning circle time series are shown in Fig.9. All simulation models predict the variation of oscillation frequency because of the change of the wave heading angle. Amplitude of the oscillation becomes larger during the beam waves and smaller during head and following waves.

Both SB-NL and SB-L underestimate the amplitude of oscillation for sway velocity and yaw rate and over predict the amplitude of the roll as shown in Fig.9. It indicates that computing wave-induced forces in the SB models used here are not good enough to predict the ship motion in waves. This is due to the assumption of low encounter frequency. Therefore SB wave models need some improvement for high encounter frequency aspects of present research using a potential flow theory with radiated and diffracted waves taken into account to predict the wave forces in head and bow waves as Yasukawa (2006a) reported. On the other hand, CFD predicts the yaw rate and roll oscillation amplitude much better than SBs. Zigzag results in waves are shown in Fig. 8b and Fig 10. In Fig.8b, EFD trajectory shows the wave drift effect while the SB models do not show it because of the deficiency of the wave model in SB. The initial surge velocity for CFD is not the same as EFD such that the wave drift effect prediction cannot be confirmed. However, it seems that the CFD overshoots as it under predicts the yaw damping. As discussed earlier, the damping under prediction might be due to not including shaft brackets and/or the simplistic propeller model. Figure10 shows the time series for 20/20 zigzag in waves. The oscillation amplitudes of EFD sway velocity and yaw rate, shown in Fig.10b and c, are much larger than that of SB motions. The CFD predicts the oscillation due to waves much better than SBs again as it includes accurately the wave diffraction forces.

System Identification

Traditionally, the system identification is used to evaluate all the maneuvering coefficients from one free-running test rather than from many captive tests. In the current work, the main object of using system identification is to investigate the mathematical model to improve the system-based predictions in waves described in Umeda et al. (2008) and Yasukawa (2006b).

The SB-NL mathematical model, shown in Eqs. (8)–(11), is used for system identification. The right-hand side shows the total forces/moments expressed as functions of the state variables and the left-hand side includes the linear, angular, Coriolis, and centripetal accelerations. In previous system identification studies, EFD free-running state variables were used to evaluate both right-hand and left-hand sides of the mathematical model. Thus, the empirical values were used to estimate some values such as the added mass and added moment of inertia. In this paper, the authors use not only CFD state variables but also total forces/moments so that the added mass and added moment of inertia can be predicted without using empirical values. Furthermore, CFD propulsion forces, rudder forces and hydrostatic forces are recorded and can be excluded from the total forces to get hull hydrodynamic forces. This makes it possible to evaluate the maneuvering coefficients and the mathematical model effectively.

Table 2 Test matrix

	Test	Fr	δ (deg)	λ / L	H / λ
Calm water	Turning Circle	0.1, 0.2	25, 35		
	Zigzag	0.1, 0.2	10/10, 20/20		
Waves	Turning Circle	0.2	35	1.2	0.02
	Zigzag	0.2	20/20	1.2	0.02

Table 3 EFD, CFD, SB-L and SB-NL turning diameters and the errors

	Fr = 0.10, δ = 25 deg	Fr = 0.20, δ = 25 deg	Fr = 0.10, δ = 35 deg	Fr = 0.20, δ = 35 deg
EFD	4.60 m	4.42 m	3.33 m	3.25 m
CFD	3.60 m (-21%)	3.44 m (-22%)	2.94 m (-12%)	3.02 m (-7%)
SB-NL	4.55 m (-1%)	4.53 m (+2%)	3.31 m (-1%)	3.30 m (+2%)
SB-L	3.38 m (-26%)	3.22 m (-27%)	2.78 m (-17%)	2.71 m (-16%)

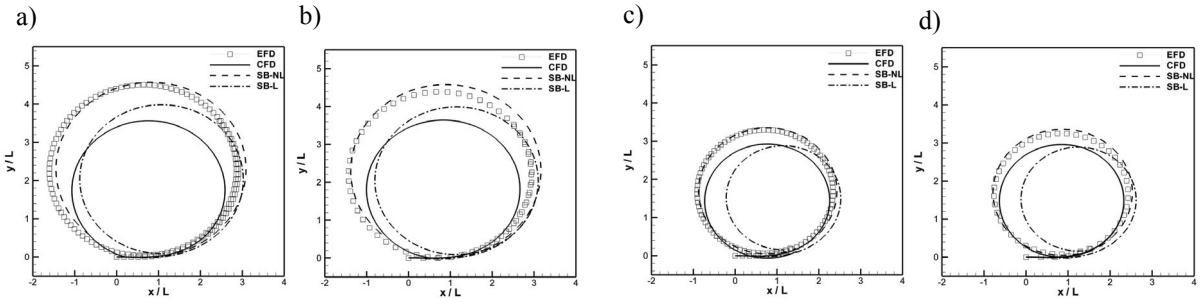

Fig.3 : Turning circle trajectories in calm water; (a): Fr = 0.10, δ = 25 deg, (b): Fr = 0.20, δ = 25 deg, (c): Fr = 0.10, δ = 35 deg, (d): Fr = 0.20, δ = 35 deg.

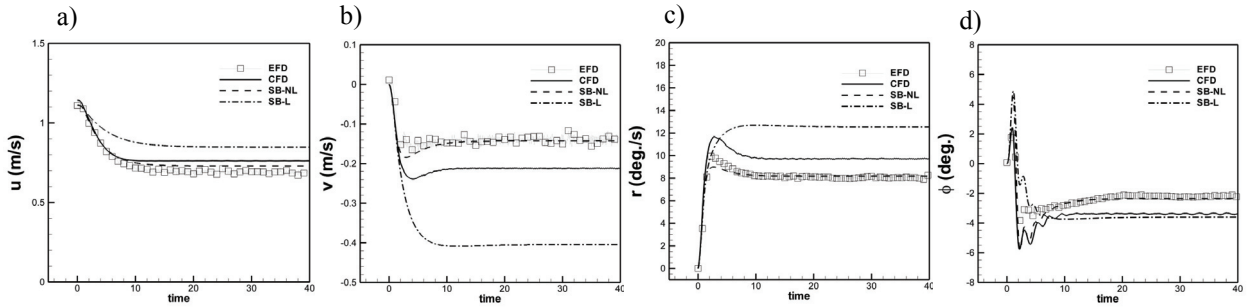

Fig.4 Time series of turning circle test in calm water with nominal Fr = 0.20, δ = 35 deg; (a): surge velocity, (b): sway velocity, (c): yaw angler velocity, (d): roll angle.

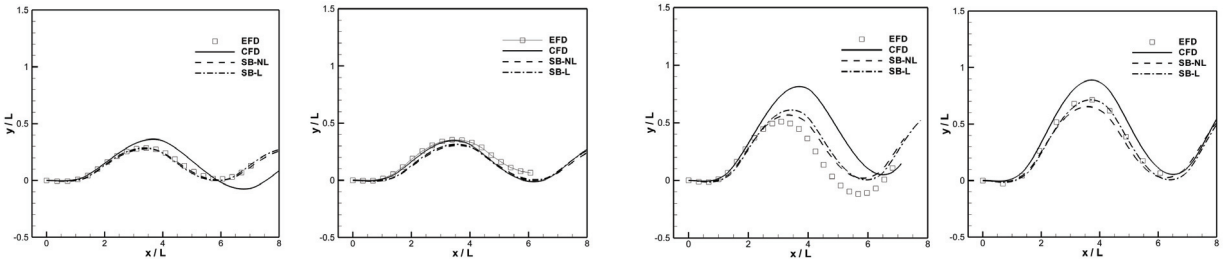

Fig.5 Zigzag trajectories in calm water; (a): 10/10 zigzag with Fr = 0.10, (b): 10/10 zigzag with Fr = 0.20, (c): 20/20 zigzag with Fr= 0.10, (d): 20/20 zigzag with Fr = 0.20.

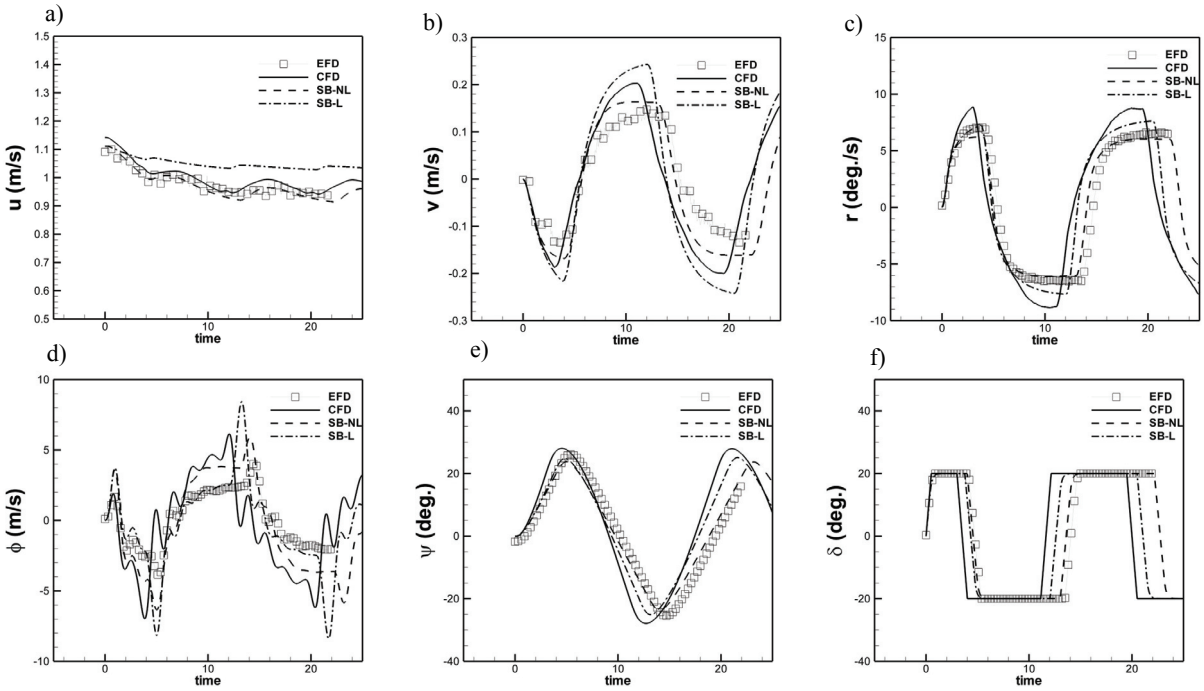

Fig.6 Time series of 20/20 zigzag in calm water test with nominal Fr = 0.20; (a): surge velocity, (b): sway velocity, (c): yaw angler velocity, (d): roll angle, e: yaw angle, (f): rudder angle.

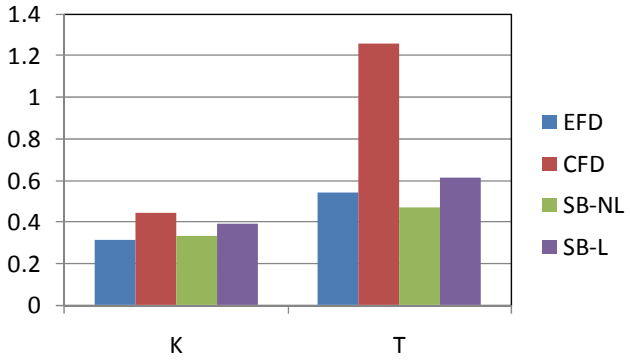

Fig.7 Comparison of steering quality indices estimated from 20/20 zigzag test in calm water with Fr = 0.20

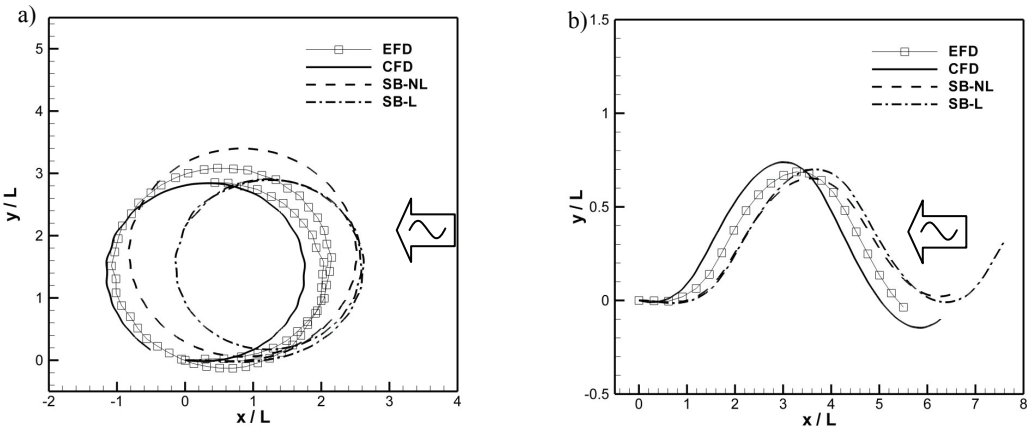

Fig.8 Trajectories in waves H/λ = 0.02, λ / L = 1.2; (a): turning circle test with nominal Fr = 0.20, δ = 35 deg, (b): 20/20 zigzag test with nominal Fr = 0.20 in waves.

a) b) c) d)

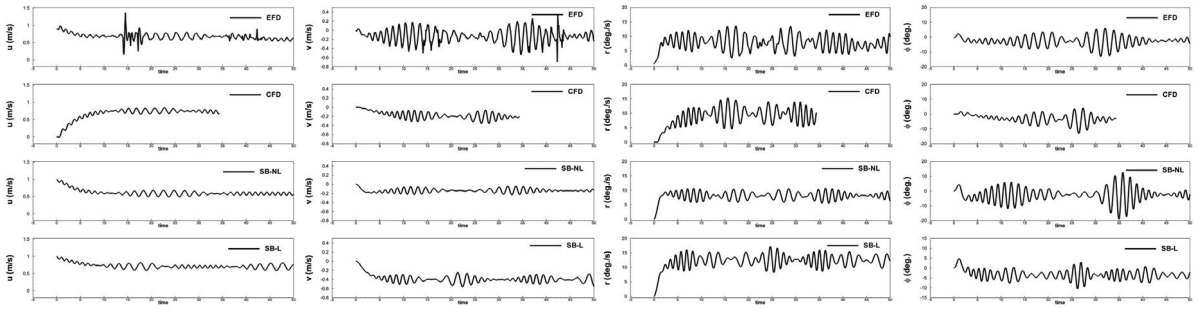

Fig.9 Time series of turning circle test in waves H/λ = 0.02, λ / L = 1.2 with nominal Fr = 0.20, δ = 35 deg; a: surge velocity, b: sway velocity, c: yaw angler velocity, d: roll angle

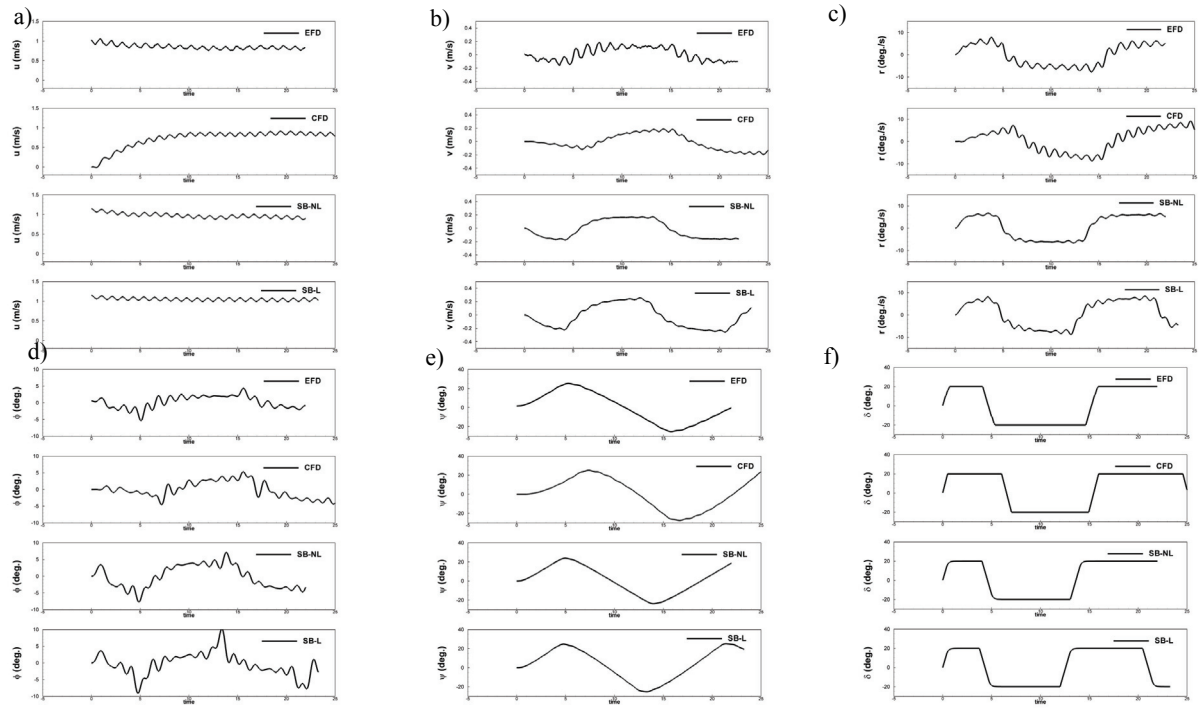

Fig.10 Time series of 20/20 zigzag in waves H/λ = 0.02, λ / L = 1.2 with nominal Fr = 0.20; (a): surge velocity, (b): sway velocity, (c): yaw angler velocity, d: roll angle, (e): yaw angle, f: rudder angle.

Least square method is the most common and simple way for the system identification. However it is known that simple least square method has difficulty to accurately predict maneuvering coefficients (Koyama et al., 1973) as some derivatives drift to the wrong values, which is known as the simultaneous drift problem (Kang et al., 1984). Since the signs of some coefficients are known from the physical meanings or empirically, as shown in Table 4, the sign constrained least square method using generalized reduced gradient algorithm (Lasdon et al., 1978) is applied. The maneuvering coefficients are computed based on the SB-NL mathematical model, shown in Eq.(5)-(8), by using CFD free-running results in calm water with Fr = 0.20. Herein the thrust, rudder forces, hydro-static forces and the resistance for x force are excluded from total forces.

Figures 11-14 show the comparison between the reconstructed maneuvering coefficients values using CFD outputs and the original values estimated from captive EFD which are used in SB-NL. The reconstructed coefficients from zigzag tests (Z20, Z10) show better agreement with EFD than those from turning circle test (T25, T35). However the discrepancy between the original values and reconstructed values are large. Previous research (Rhee and Kim, 1999) showed that the turning circle and zigzag tests are not effective enough to avoid the simultaneous drift problem in

which the role of each component cannot be distinguished. Therefore the other types of maneuvering such as sinusoidal rudder test and random rudder test might have better results as they produce unsteady sway and yaw motion, which helps avoid simultaneous drift problem. The very large angle zigzag test proposed by Rhee and Kim (1999) also shows better estimation than other conventional tests. Better system identification techniques such as extended Kalman filtering (Lewis, 1986) or using outputs of several free-running simulations, so called parallel processing (Abkowitz, 1980), might also improve the prediction of maneuvering coefficients. For the wave cases, there is a chance to predict the maneuvering coefficients if the wave-induced forces can be removed from the total forces.

Table 4 Constrain for maneuvering coefficients

Maneuvering coefficients	sign
$m_x, m_y, J_{xx}, J_{zz}, X_{vr}, K_r, K_v$	≥ 0
$X_{rr}, X_{vv}, Y_r, Y_v, K_p, N_r, N_v$	≤ 0

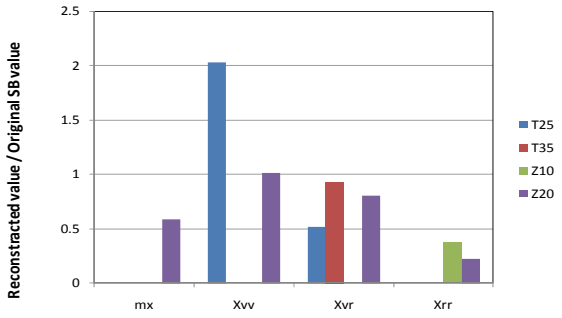

Fig.11 Reconstructed maneuvering coefficients ratio for surge; (T25) turning circle with δ = 25 deg, (T35) turning circle with δ = 35 deg, (Z10) 10/10 zigzag, (Z20) 20/20 zigzag.

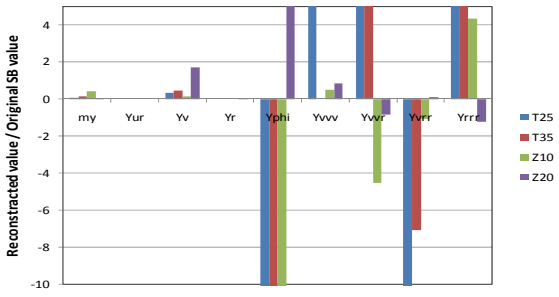

Fig.12 Reconstructed maneuvering coefficients ratio for sway.

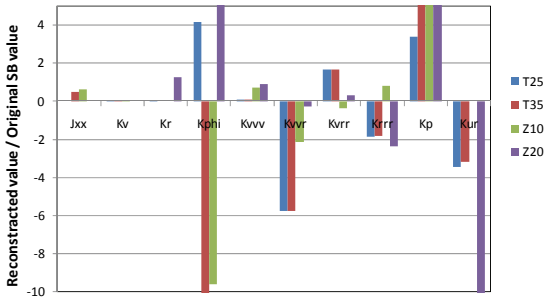

Fig.13 Reconstructed maneuvering coefficients ratio for roll.

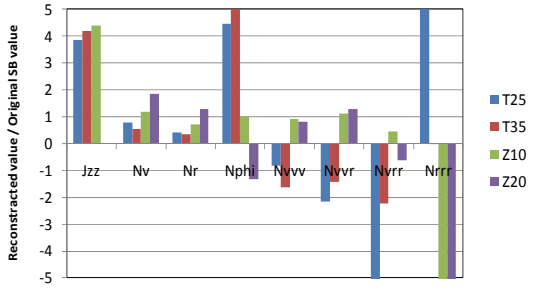

Fig.14 Reconstructed maneuvering coefficients ratio for yaw.

CONCLUSIONS AND FUTURE WORKS

Free-running tests in calm water and waves are executed in the IIHR wave basin. The tests are simulated by CFD and SB. Both CFD and nonlinear SB simulation show enough ability to predict calm water maneuvers. However, the SB models could not predict the shifting in the turning circle in waves as SB models do not include any of the wave drift force terms. CFD results also showed that the CFD overshoots the EFD courses in zigzag and under predicts the turning diameter in turning circle simulations. The maneuvering coefficients in SB-NL model are predicted by using CFD state variables and forces. However the sign constrained least square method could not solve the simultaneous drift problem.

In future, SB models focusing on high-frequency phenomena also would be applied to predict the wave forces. CFD also needs to be improved by including all appendages in the CFD model and possibly improving the propeller model. In addition, other types of calm water maneuvering such as random rudder deflection test, sinusoidal rudder test or very large angle zigzag test should be used for system identification. Moreover, better

system identification techniques such as extended Kalman filtering or parallel processing will be taken into account for the future work. For EFD, a launching system, guiding system and local flow measurement system in experiment will be installed to improve the tests. An imaged-based non-contact type motion measurement system will be prepared to get more precise motion data. In addition, to enhance tracking performance of carriage at tests in waves, modification of tracking system such as low-pass filtering of feedback signal is now under consideration.

ACKNOWLEDMENTS

The research performed at IIHR was sponsored by the US Office of Naval Research, grants N00014-01-1-0073 and NICOP N00014-06-1-064 under administration Dr. Patrick Purtell. The CFD simulations were conduced utilizing DoD HPC.

REFERENCES

Abkowitz M. A. (1980), "Measurement of Hydrodynamic Characteristics from Ship Maneuvering Trials by System Identification", Advance Copy of Paper, Annual Meeting of SNAM.

Carrica, P.M., Huang, J., Noack, R., Kaushik, D., Smith, B., Stern, F. (2010), "Large-scale DES computations of the forward speed diffraction and pitch and heave problems for a surface combatant", Computer &Fluids, vol. 39, Issue 7, pp. 1095-1111.

Carrica P. M., Ismail F., Hyman M., Bhushan S. Stern F. (2011), "Turn and Zigzag Maneuvers of a Surface Combatant Using a URANS Approach with Dynamic Overset Grids", submitted to J. of Ocean Engineering.

Fujii H. and Tuda T. (1961), "Experimental Researched on Rudder Performance. (2)", J. of Zousen Kiokai, Vol.110 (in Japanese).

Hashimoto H., Stern, F., and Sadat Hosseini, S. H. (2008), "An Application of CFD for Advanced Broaching Prediction (2ndReport)", Proc. Conf. of the Japan Soc.of Naval Architects and Ocean Eng., Vol. 6, pp. 237-240.

Kang, C.G., Seo, S.H., Kim, J.S., 1984, "Maneuverability Analysis of Ship by System Identification Technique",SNAK ,vol.21, No.4.

Koyama, T., Watanabe, T., Watanabe, I., (1973), "An Application of the Least Square Method to the Ship Maneuverability Identification", Proc of the Symp. on Maneuverability, the Soc. of Naval Architects of Japan, vol.134, pp.173-181.

Lasdon S. L. et al. (1978), "Design and Testing of a Generalized Reduced Gradient Code for Nonlinear Programming", J. of ACM Trans on Math Software, Vol. 4 Issue 1.

Lewis F. L., (1986), Optimal Estimation –with an introduction to stochastic control theory, John Wiley & Sons, Inc.

Nomoto K., Taguchi K., Honda K. and Hirano S. (1956), " On the Steering Qualities of Ships", J. of Zousen Kiokai, vol.99, pp.75-82 (in Japanese)

Rhee K. P. and Kim K.(1999)," A new sea trial method for estimating hydrodynamic derivatives", Ship & Ocean Technology Vol.3, Issue 3, pp. 25–44.

Sadat-Hosseini, H., Stern, F., Olivieri, A., Campana, E., Hashimoto, H., Umeda, N., Bulian, G., Francescutto, A. (2010), "Head-waves parametric rolling of surface combatant", J. of Ocean Eng. Vol. 37, Issue 10, pp 859-878.

Sadat-Hosseini H. et al. (2011), "CFD, system-based and EFD study of ship dynamic instability events: surf-riding, periodic motion, and broaching", J. of Ocean Eng., Vol. 38, Issue 1, pp. 88-110.

Umeda N. (2000), "Application of nonlinear dynamical system approach to ship capsize due to broaching in following and quartering seas". In: Vassalos D, et al. (eds) Contemporary ideas on ship stability. Elsevier, Amsterdam, pp 57–68.

Umeda N., Yamamura S. et al (2008), "Extreme Motions of a Tumblehome Hull in Following and Quartering Waves", Proc. of the 6th Osaka Colloquium on Seakeeping and Stability of Ships, Osaka, pp.437-443.

Yasukawa H. (2006a), "Simulation of Wave-Induced Motions of a Turning Ship", J. of the Japan Society of Naval Architects and Ocean Eng, Vol. 4, pp.117-126 (in Japanese).

Yasukawa H. (2006b), "Simulation of Ship Maneuvering in Waves (1st report: turning motion)", J. of the Japan Society of Naval Architects and Ocean Eng, Vol. 4, pp.127-136 (in Japanese).